T.1: Pinger magnet system in Indus-2

Gangopadhyay Sampa[1], Pareek Prashant[2], Singh Yash Pal[3], Tyagi Deepak Kumar[4], Vikas[5], Yadav D.P.[6], Yadav Surendra[7], Puntambekar T.A.[8*]

[1]*Accelerator Control Systems Division*
[2]*Accelerator Magnet Technology Division*
[3]*Accelerator Power Supplies Division*
[4]*Accelerator Physics Section*
[5]*Indus Operation Division*
[6]*Ultra High Vacuum Technology Section*
[7]*Beam Diagnostics & Coolant Systems Division*
[8]*Electron Accelerator Group*
[*]*Email: tushar@rrcat.gov.in*

Abstract

A pinger magnet system consisting of two kickers, one for each transverse plane, has been commissioned at Indus-2 synchrotron radiation source. The main components of vertical and horizontal pinger magnet system are pulsed pinger magnets, alumina ceramic vacuum chambers, pulsed power supplies, beam position indicators (BPIs) and control system. These kickers excite betatron oscillations on electron beam in order to probe the linear and non-linear beam dynamics regime together with the turn-by-turn beam position measurement capabilities of the BPIs in Indus-2 storage ring. The pulse magnets have been mounted around a very thin titanium coated ceramic vacuum chamber. The vertical pinger magnet produces 958 ns wide half sinusoidal magnetic field capable of generating a peak value of 650 gauss at 5.5 kA peak driving current. The horizontal pinger magnet produces half sinusoidal 596 gauss peak field at 2.7 kA peak current. These pulse excitations are sufficient to deliver required kick of 2 mrad and 1.5 mrad for vertical and horizontal pinger magnets, respectively. In the preliminary experiments performed, turn-by-turn beam position data was collected using the vertical pinger magnet and analyzed for extracting the information related to linear beam optics in Indus-2. This theme article presents brief description of the various components of the pinger magnets and the initial experimental results of some of the basic beam parameters measured using pinger magnet system.

1. Introduction

When a storage ring is operational, fast and accurate measurement and correction of its lattice parameters becomes important in order to bring the storage ring performance close to the theoretical model in respect of linear as well as nonlinear behaviour. With the analysis of turn-by-turn (TBT) beam position data acquired after applying a transverse kick to the beam using a "Pinger magnet", linear and nonlinear studies of the lattice parameters (such as betatron tune, betatron function and phase, beta-beat, phase space, betatron coupling, dynamic aperture, resonance driving terms, frequency map analysis etc.) can be carried out [1]. Indus-2 is a synchrotron radiation (SR) source of 2.5 GeV energy / 200 mA stored current operating at RRCAT, Indore in round-the-clock mode. In order to understand and improve the performance of Indus-2, there is a need to carry out linear and nonlinear studies of the lattice parameters. Also, in future, it is envisaged to operate Indus-2 with low emittance beam and then measurement of nonlinear optics and its correction through the suppression of resonance driving terms using harmonic sextupole magnet will be essential part of beam dynamics optimization. Keeping this in view, two pinger magnets have been installed in Indus-2 storage ring, which will be useful to measure the optics parameters in both the planes. Pinger magnet is pulsed dipole magnet, which deflects the beam in transverse plane during one turn circulation around the ring. After the deflection, the beam oscillates about the closed orbit and the beam position indicators (BPIs) record the position of beam centroid turn after turn. The main components of vertical and horizontal pinger magnet system consist of pinger magnets, vacuum chamber, pulsed power supplies, beam diagnostic devices and control system. Brief description of the various components of pinger magnet system is given in the following sections.

2. Pinger magnets [2]

Before finalizing the design parameters of the pinger magnet, the available space in Indus-2 lattice was identified. In the long straight section 4 (LS-4), 330 mm space was available while 350 mm was available in short straight section 7 (SS-7). No empty space was available where both the magnets could be placed adjacently. The maximum length of the pinger magnet, which could be accommodated at these locations was ~ 250 mm. The maximum deflection angle provided by the pinger magnets was calculated such that the dynamic aperture can be probed up to the physical limit of the vacuum chamber that depends on the beta function at these locations in both the planes. The maximum kick required for the horizontal and vertical pinger magnet was calculated to be 1.5 mrad and 2.0 mrad, respectively. It was decided to install horizontal pinger magnet in LS-4 and vertical pinger magnet in SS-7 section of Indus-2 lattice. The examined bunch train should experience the kick only once per revolution. For this purpose, the pulse length of the pinger magnet must be less than the revolution time (575 ns) in Indus-2. Due to the difficulty faced by the power supply design to discharge high voltage capacitor in such a short period, it was decided to increase the pulse width of pinger magnet. From the beam dynamics point of view, the pulse length of the pinger magnet was kept of the order of 1 μs, which is shorter than twice the revolution time. With properly setting the delay and trigger of the pinger magnet, the beam will experience the kick only once in one revolution time. Figure T.1.1 shows vertical and horizontal pinger magnets installed in Indus-2. These are pulsed dipole ferrite core magnets, which produce half sinusoidal magnetic field for about less than 1 μs.

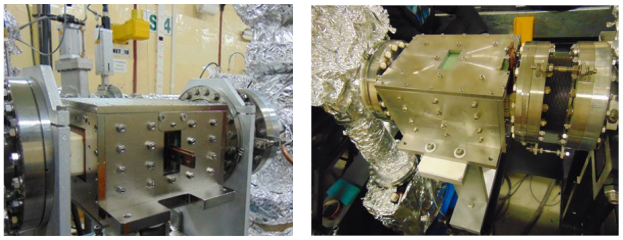

Fig. T.1.1: Vertical and horizontal pinger magnets installed in Indus-2.

The vertical pinger magnet produces 958 ns wide half sinusoidal magnetic field having a peak value of 650 gauss at 5.5 kA peak current. The horizontal pinger magnet produces half sinusoidal 596 gauss peak field at 2.7 kA peak current. Pulse width of pulse magnetic field is 948 ns. The pulse magnetic field uniformity achieved along pole width and pole gap is better than ±2 x 10^{-3} in good field region for both the magnets, which are shown in Figure T.1.2 and Figure T.1.3, respectively.

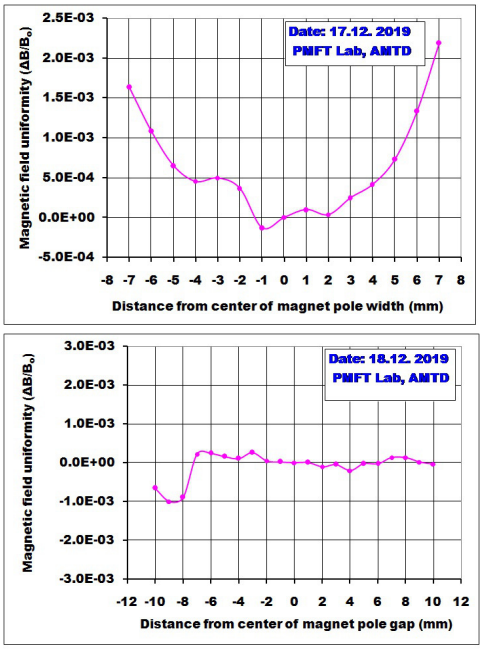

Fig.T.1.2: Magnetic field uniformity of vertical pinger magnet along pole width and pole gap.

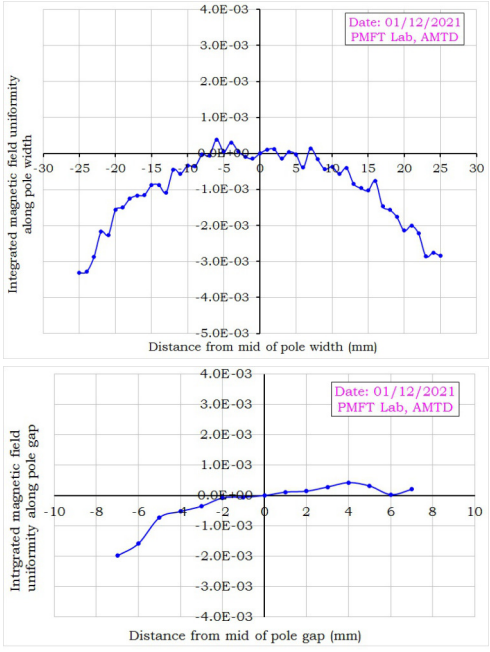

Fig. T.1.3: Magnetic field uniformity of horizontal pinger magnet along pole width and pole gap.

The main challenges involved in the development of these magnets were minimization of magnet inductance to achieve half sinusoidal magnetic field pulse of less than 1 μs, optimization of Ti coating thickness inside the ceramic chamber to keep the magnetic field delay and the heating due to image current within limits, and handling the high voltages between various components of the magnet [3].

3. Pinger magnet power supplies

Two pulsed power supplies are required to energise vertical and horizontal pinger magnets. Half sine current pulse with peak currents of 5500 A and 2700 A, respectively and pulse width < 1 μs were required to energize these magnets to generate required deflection. The power supply specifications stipulated use of low-inductance, high voltage capacitor switched pulser with thyratron as a switch to meet the requirements. As the working voltage had to be reduced to a minimum, it was obvious to reduce the path inductance. Efforts were made to reduce path inductance of pulse power circuit in order to meet this objective by way of designing of coaxial thyratron assembly, pulse forming network (PFN) with low equivalent series inductance (ESL) capacitors and positioning PFN near the pinger magnet. Considering the design working voltages and high *di/dt* of currents, thyratron was selected as the high voltage switch for this application. The design was specifically tailored for low jitter, high *di/dt* load current and to deal with the problems of slow recovery and reverse arcing associated with the thyratron switch. The schematic of pulse power circuit is shown in Figure T.1.4.

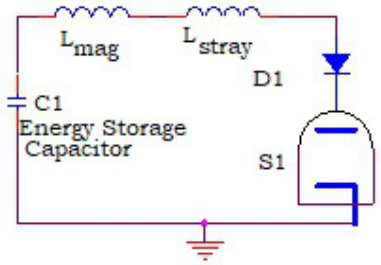

Fig. T.1.4: Pulse power circuit.

Value of capacitor C1 is 130 nF and 80 nF for vertical and horizontal pinger power supplies, respectively. Low ESL capacitor (C1) is charged to high voltage using a command resonance charging scheme. A resistive charging scheme is used to charge the low voltage capacitor. A feedback loop controls the voltage across the capacitor. Consideration has been given to high voltage safety and long operational life while designing the pulse power circuit and it's switching circuit. In pinger power supplies, the amplitude of current pulse is set by remote reference from the control room. Both current peak and pulse width are determined by C1 and total path inductance (L_{mag} + L_{stray}). In the highly underdamped circuit, firing switch S1 (thyratron) generates a pulsed half sine current pulse. Fast current monitor is used to measure the current pulse. The supplies were built on site in custom built racks and tested for all the specifications with installed pinger magnet. Control of the power supplies was performed remotely from Indus-2 control room, while load current pulse

was transmitted to control room for monitoring and experimentation. Figure T.1.5 depicts the current waveform of horizontal pinger magnet. Figure T.1.6 shows the installed pulse power circuit near the horizontal pinger magnet and Figure T.1.7 shows the commissioned power supply. Figure T.1.8 depicts the current waveform and lagging magnetic field of vertical pinger magnet. Figure T.1.9 shows the installed pulse power circuit near to vertical pinger magnet and Figure T.1.10 shows the commissioned power supply. To realize magnetic field pulse width less than 1 µs, current pulse width was designed for 954 ns in vertical pinger magnet and 878 ns for horizontal pinger magnet. The same is seen in respective pulse current waveforms.

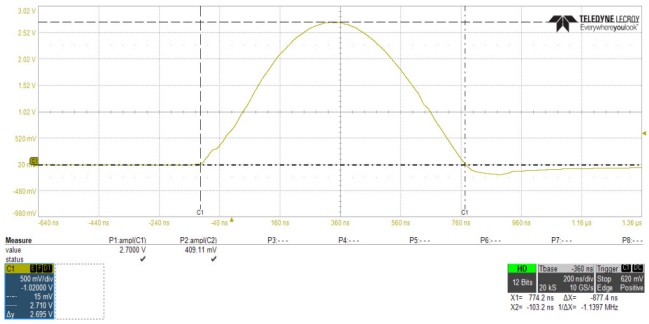

Fig. T.1.5: Magnet current waveform.

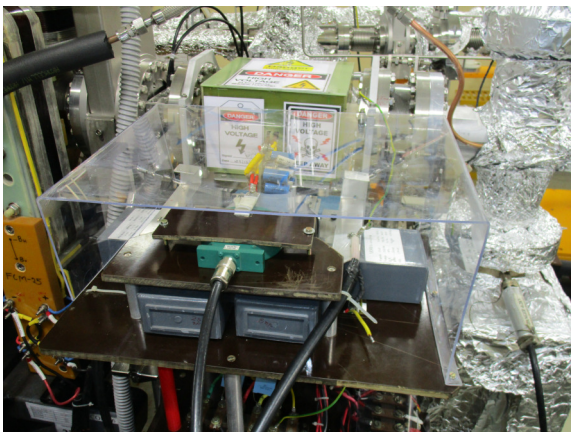

Fig. T.1.6: Photograph of pulse forming network.

Fig. T.1.7: Commissioned power supply in Indus-2.

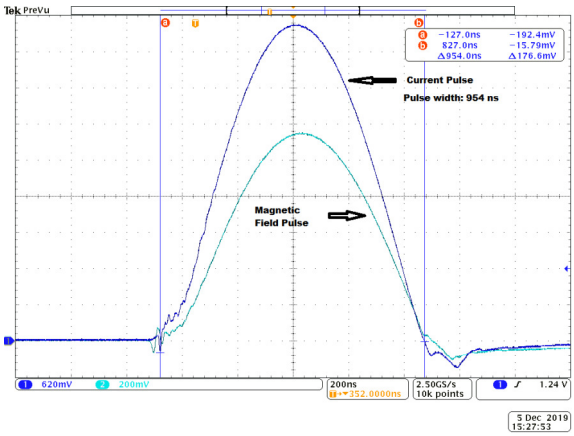

Fig. T.1.8: Vertical pinger magnet power supply current and field waveform.

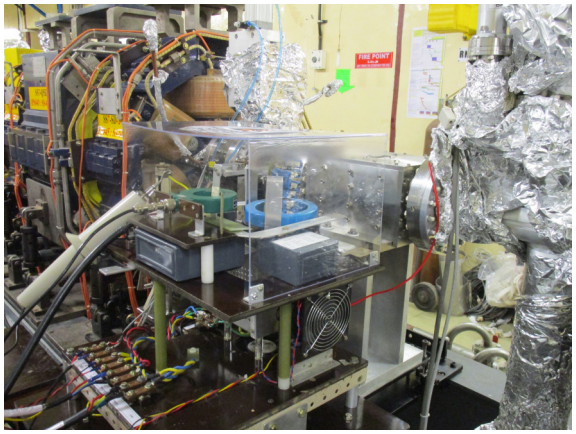

Fig. T.1.9: Vertical pinger magnet power supply PFN.

Fig. T.1.10: Commissioned vertical pinger power supply.

4. Vacuum chamber for pinger magnets

Since the pinger magnet is a fast pulsed magnet, it can't be mounted on the metallic pipe, as it shields the fast changing magnetic field. A vacuum chamber made of ceramic is necessarily used for such elements [2, 4]. It also reduces the heating due to eddy currents. However, a thin conductive coating is provided inside this chamber due to following reasons: (1) to avoid the electrical discontinuity of the chamber and to provide path for flow of the image current of the beam, (2) to prevent the static charge built up on the ceramic surface, and (3) to shield the stored beam from ceramic and ferrite at high frequencies to avoid possible resonances. Generally, titanium (Ti) is used as a coating material due to its known properties of high resistivity, high melting point and good adhesion with ceramic. Such coating inside the chamber again shields the magnetic field and causes heating of the chamber walls due to eddy currents. These contradictory requirements make the optimization of the coating thickness critical. The thickness of the coating has been evaluated on the basis of permissible field attenuation, beam deposited power and magnet excitation deposited power. It was decided to keep the Ti coating thickness of 500 nm. In Figure T.1.11, the effect of the Ti coating on the pinger magnet pulse is shown. Field attenuation and time shift of the pinger magnet peak field due to coating are tabulated in Table T.1.1.

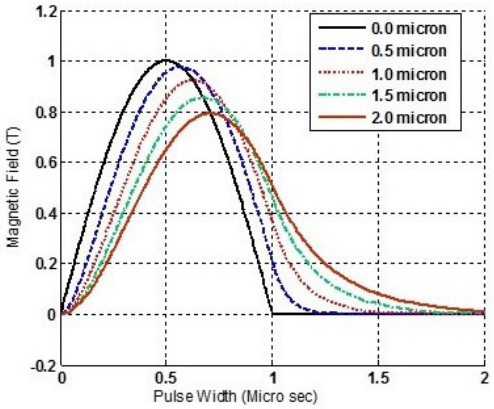

Fig. T.1.11: Pinger magnet pulse signal attenuation versus coating thickness.

The graph above and data in Table below has been arrived at on the basis of theoretical calculations.

Table T.1.1: Pinger magnet pulse attenuation and time delay due to different coating thicknesses.

Coating thickness (µm)	Field attenuation (%)	Time delay (ns)
0.5	2.25	70
1.0	7.83	125
1.5	14.4	170
2.0	20.7	210

Two nos. of precision alumina ceramic ultra-high vacuum (UHV) chambers with titanium coating onto vacuum exposed surface were designed and indigenously developed with partial support from Indian industry, tested and installed inside fast pulsed vertical and horizontal pinger magnets in Indus-2 storage ring. Vertical and horizontal pinger magnet systems along with associated UHV systems were installed in SS-7 and LS-4 straight sections of Indus- 2 during December 2019 and December 2021, respectively. The vacuum chamber is made of high purity (99.7%) alumina to mitigate the issue of eddy current effects in case of metallic chamber due to time varying magnetic field. Active brazing technique was used to join alumina to Kovar® rings. Kovar ring to SS316L end flange joint was accomplished by autogenous DC TIG (manual) in case of vertical pinger chamber and by fiber coupled pulsed Nd:YAG laser welding (mechanized) in case of horizontal pinger chamber [5]. TIG and laser welding were carried out at RRCAT. Titanium coating of ~ 0.5 µm thickness onto vacuum exposed surface of the chamber provides electrical continuity for the image current and it is sufficiently thin to generate insignificant eddy current having negligible effect on the generated pulsed magnetic field of pinger magnets. Salient design features of the alumina ceramic chamber are: iso-statically pressed, sintered and ground monolithic flanged alumina tube, flatness and parallelism of ferrite mating outer surfaces within 100 µm, ceramic-to-metal joint free from tensile loading, RF continuity, reduced torque for He leak tight metal sealing and UHV compatibility. Active brazing technique was used for direct brazing of Kovar® to alumina joint. Helium leak-tightness of the brazed alumina to kovar and kovar to SS316L welded joint was confirmed with helium tuned mass spectrometer leak detector (HMSLD) with background helium leak rate of $<2 \times 10^{-10}$ mbar.l/s, before and after bake-out at 150 °C for 48 hours. Photograph of the fully assembled alumina chamber is shown in Figure T.1.12. Titanium coating of the alumina tube was developed using in-house magnetron sputtering facility. The photograph of coating facility integrated with alumina chamber for coating is shown in Figure T.1.13. The process parameters for the coating were optimized by multiple trials on samples to obtain good repeatability of the coating quality.

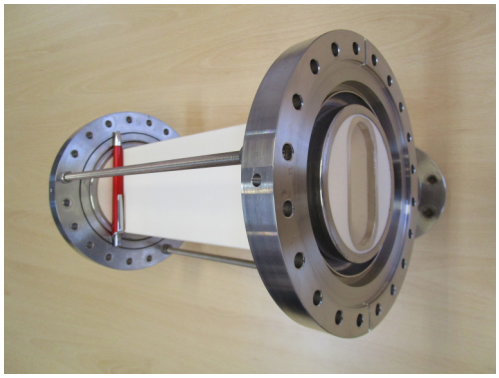

Fig. T.1.12: Alumina UHV chamber assembly.

The measured thickness of Ti coating on final chamber was found to be within the desired range of 0.5 µm ± 20%. Coated chamber was subjected to thermal cycling twice from room temperature – 150 °C - room temperature and no peel-off/swelling of coating was observed.

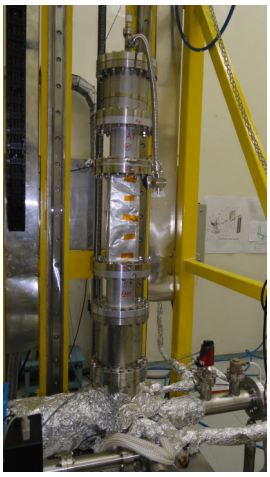

Fig. T.1.13: Coating facility integrated with alumina chamber for coating.

Photograph of uncoated and coated condition end views of the chamber is shown in Figure T.1.14(a) & T.1.14(b), respectively. Prior to installation, both the coated chambers were tested for their UHV and magnetic pulse compatibility and test results were found in conformity with the requirements. Subsequent to installation and after bake-out at 150 °C for 48 hours, ultimate vacuum of ~5 x 10^{-10} mbar was achieved in the ring within stipulated shutdown time schedule. Both the chambers are performing well in Indus-2 since their installation.

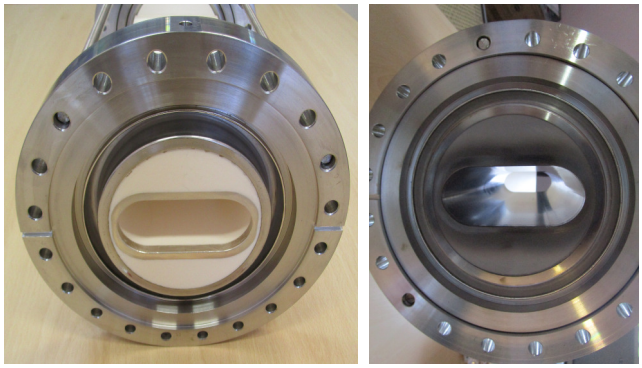

(a) (b)

Fig. T.1.14: Alumina chamber end views- (a) before, and (b) after Ti coating.

Photographs of the installed chambers in Indus-2 are shown in Figure T.1.15 and Figure T.1.16, respectively. The fully "Make in India" product is a vital import substitute for Indian accelerator program.

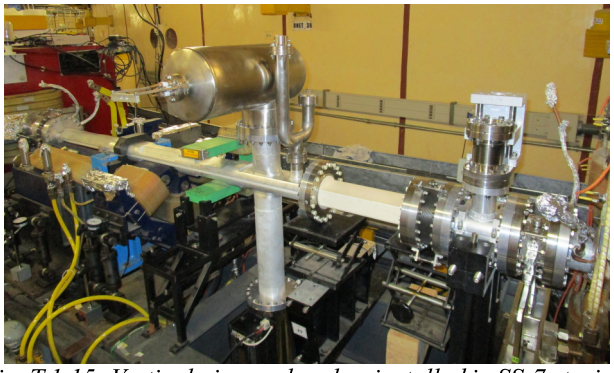

Fig. T.1.15: Vertical pinger chamber installed in SS-7 straight section (December 2019).

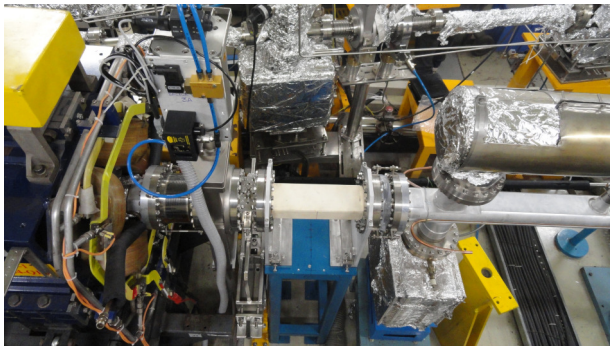

Fig. T.1.16: Horizontal pinger chamber installed in LS-4 straight section (December 2021).

5. Alignment of pinger magnets

In both the sections, before start of opening of the vacuum envelope for installation, coordinates of references over position-sensitive components were measured and recorded. Multiple sessions of measurement were done to guide installation of whole vacuum envelope. Finally, precise alignment of ceramic vacuum chambers passing through the pinger magnets (horizontal & vertical) is prerequisite for correct alignment of respective pinger magnets. Laser tracker was used for 3D coordinates and optical level for precise elevation. Elevation was directly measured over smooth ferrite slabs of pinger magnets, whereas for alignment in horizontal plane, magnets were provided with precisely known values of offsets with respect to their center-line. After completion of installation, alignment of pinger magnets in horizontal plane was better than 0.2 mm with respect to the best-fit line (reference line) passing through the references of quadrupoles of corresponding sections. Elevation was better than 0.15 mm with respect to bench mark of elevation.

6. Pinger magnet control system

Indus-2 timing control system (TCS) caters to supervision, monitoring and timing synchronization aspects of various pulsed devices and measuring setups used in Indus-2. Indus-2 TCS has now been enhanced to provide for the new control and timing synchronization requirements for operating two more pulsed magnets, namely vertical and horizontal pinger magnets in Indus-2. Indus-2 TCS facilitates remote operation of Pulsed Power Supplies (PPSs) for pulsed magnets like

kicker and septum to extract the beam from Booster and inject the electron beam into Indus-2 ring. The remote operation includes control, monitoring and triggering. Pinger magnets require similar control system in addition to some stringent timing trigger requirement. Hence, Indus-2 TCS is augmented to accommodate the electronics for controlling the PPSs for pinger magnets remotely.

Indus-2 TCS has three layer architecture with VME (Versa Module Euro card) bus based controllers at Layer-2 (L-2) and Layer-3 (L-3) [6]. Layer-1 (L-1) is the SCADA based Application Program layer, L-2 is the supervisory control (SC) layer with real time operating system OS-9 (RTOS-OS9) on MVME-162 CPU. L-3 is the equipment control (EC) layer. On this layer, hardware comprises of VME input / output (I/O) boards, trigger generator boards, RTOS-OS9 based Motorola 68000 VME CPU and Profi slave board for communication to Profi Master at Layer-2 station. L-1 and L-2 communicate over 100 Mbps Ethernet [6]. Indus-2 TCS has been augmented by including new hardware and updating software at all the three layers for new signals of pinger magnets. New I/O boards have been introduced in the equipment control station (ECS). Various signals for pingers have been added.

A new field programmable gate array (FPGA) based VME [A24:D16] trigger generator board (Figure T.1.17) is developed. It is a multi-channel configurable trigger signal generator board. Delay of each trigger channel is remotely adjustable in coarse and fine time scale with respect to the on-board generated start pulse. Trigger signals are synchronized to Indus-2 revolution clock at 1.73 MHz, which is derived on-board from the Indus-2 RF signal at 505.8 MHz. Delay resolution is 0.5 ns and timing jitter is < 1 ns among the channels (Figure T.1.18). The trigger pulses are interfaced with field devices using channel-to-channel isolation. Trigger isolator board has been developed for isolating the trigger pulses for different field devices. Optical fibre based trigger signal interface electronics is also implemented for main trigger pulses of PPSs. VME I/O boards are added for monitoring & control of various digital and analog signals. New analog channels are added with 4-20 mA current signal interface and channel-to-channel isolation for reference setting and read-back signals. Augmented ECS of Indus-2 TCS with new hardware is shown in Figure T.1.19. Embedded programs at Layer-2 and Layer-3 have been modified to handle additional data and commands to access the new I/O boards for new analog and digital I/O signals. OS-9 based driver firmware is developed for new trigger board. The WinCCOA SCADA based Application Program Interface (API) has been updated at Layer-1. Existing graphical user interface (GUI) program is enhanced by adding the new GUI panel (Figure T.1.20) for pinger magnets. It supports control/monitoring of I/O parameters, delay settings for trigger pulses to PPSs and beam position indicator (BPI) in coarse and fine time scale, selective triggering to operate the required pinger magnets, choosing the operating modes like single trigger or continuous trigger at 1 Hz, etc. Data logging and web display of parameters have been implemented.

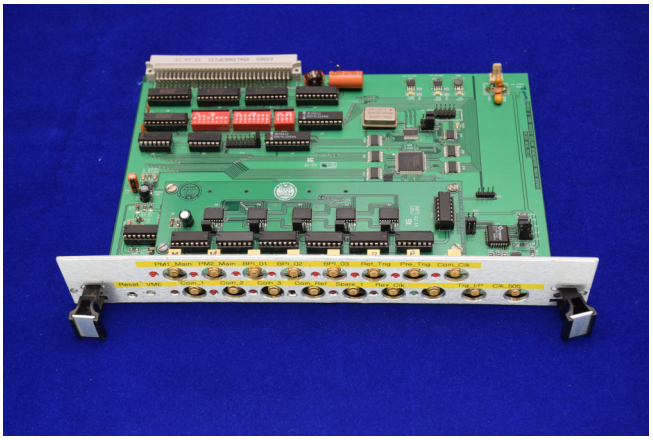

Fig. T.1.17: Multi-channel VME trigger generator board.

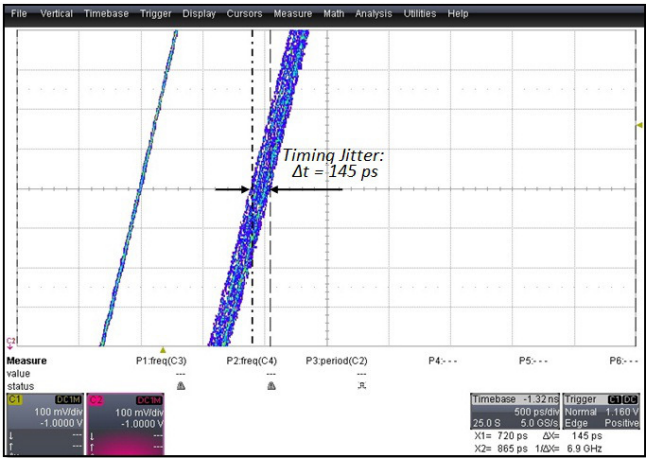

Fig. T.1.18: Channel-to-channel jitter of 145 ps.

Full implementation, integrated testing of the new hardware & software and system commissioning has been done in two phases. Vertical pinger magnet was made operational remotely in the first phase prior to horizontal. PPSs for vertical and horizontal pinger magnets are interfaced with the new control hardware and are remotely operated successfully along with pinger magnets at full load.

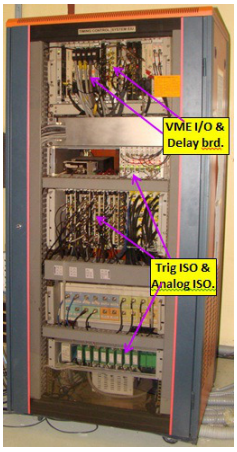

Fig. T.1.19: Augmented ECS with new hardware.

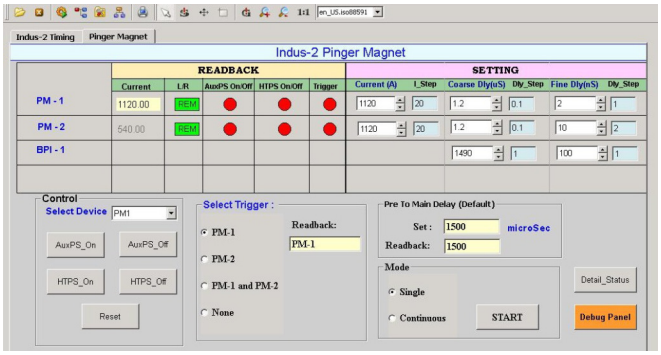

Fig. T.1.20: GUI panel for pinger magnet control.

7. Measurement and analysis of TBT beam position data in Indus-2

For beam dynamics studies, the pinger magnet is excited with an electric current pulse to exert a transverse kick on the electron beam for a period of time less than two revolution periods of the beam. In synchronization with pinger magnet excitation, turn by turn (TBT) beam position data is measured using the beam position indicators (BPI) distributed on the Indus-2 ring. In Indus-2, out of 56 BPIs, 14 BPIs have the capability to measure and store turn-by-turn beam position data. A trigger signal (PM_trigger) obtained from the trigger signal of the pinger magnet's power supply has been used during the acquisition of turn-by-turn beam position data for synchronization with the pinger magnet excitation [7]. The pinger magnet can be excited to deliver repetitive or a single kick to the beam.

A small number of bunches in the beam with sufficient stored beam current is required in the experiment with pinger magnet, so that all bunches are coherently excited by the pinger magnet and corresponding responses of the BPIs are proper [8]. During the experiment in Indus-2, electron beam of 32 bunches (the minimum number of bunches that can be set in the software in single bunch train mode) were filled. Thereafter, bunches were cleaned with the help of bunch cleaning system, which reduced the number of filled bunches to 10. After this, the energy of the beam of 10 bunches was increased to 2.5 GeV. The vertical pinger magnet was then excited to exert a single kick to the beam. In synchronization with the excitation, turn-by-turn beam position data from all the 14 BPIs were acquired using an in-house developed software and recorded in PC. The experiment was repeated for different peak current settings of the vertical pinger magnet power supply and the corresponding TBT data were recorded.

A very first and preliminary analysis of TBT data was carried out in order to extract basic parameters related to linear beam optics. In Figure T.1.21, TBT data captured at BPI-6 is shown in vertical plane (a) and in horizontal plane (b). Though the kick is applied in vertical plane, due to betatron coupling and BPIs tilt etc., the amplitude signal in horizontal plane was also observed.

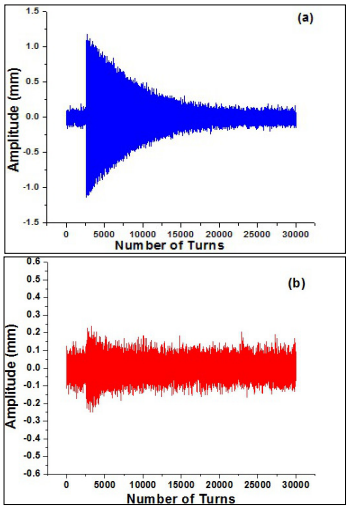

Fig. T.1.21: TBT data in (a) vertical plane, and (b) horizontal plane at BPI-6 of Indus-2.

When the beam undergoes coherent betatron oscillations, the turn-by-turn beam orbit seen by a BPI is the discrete sampling of a sinusoidal signal. The TBT orbit data at the i^{th} BPI is represented as

$$x_i(n) = A_i sin(2\pi\nu n + \psi_i + \chi)$$

where, n is the turn number, A_i and ψ_i are the oscillation amplitude and phase at the BPI, ν is the fractional part of betatron tune and χ is the phase constant. Applying the harmonic analysis, the amplitude and phase of these oscillations at each BPI can be given by [9]

$$A_i = \frac{2}{n}\sqrt{C_i^2 + S_i^2} \;\&\; \psi_i = tan^{-1}\left(\frac{C_i}{S_i}\right)$$

where, $C_i = \sum_{i=1}^{n} x_i(n)cos(2\pi\nu n)$, and
$S_i = \sum_{i=1}^{n} x_i(n)sin(2\pi\nu n)$.

7.1 Betatron tune

The first parameter, which is calculated using measured TBT data is betatron tune. The Fourier transform of the TBT data shows that there is a largest peak, which corresponds to fractional part of betatron tune in both the planes (Q_x / Q_y = 9.2/6.2). The other two peaks in the horizontal plane spectra are seen near 0.3 and 0.4, those are a signature of sextupole driven and quadrupole driven resonances. Though their amplitudes are not large enough to affect the beam severely, the initial fast Fourier transform (FFT) results are shown in Figure T.1.22 and more rigorous analysis is in progress.

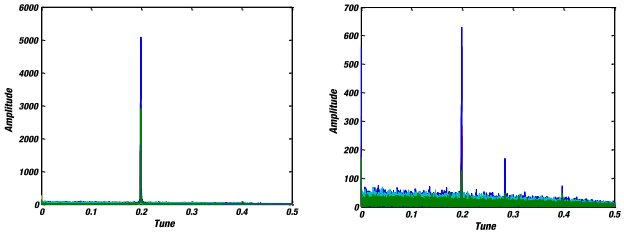

Fig. T.1.22: FFT results of TBT BPI data in Indus-2.

7.2 Phase space

The transverse phase space coordinates of an orbit can be derived from BPI measurement at two locations if the transfer matrix between those locations is known. In the simplest case, two BPIs are separated by only a drift space, the angle coordinates are

$$x'_{1,2} = {(x_2 - x_1)}/{L}, y'_{1,2} = {(y_2 - y_1)}/{L}$$

Where $x_{1,2}$ & $y_{1,2}$ are the horizontal and vertical positions measured at BPIs 1 and 2, respectively, with BPI 1 located upstream of BPI 2, and L is the length of the drift space. From the TBT data, we have constructed the phase space at BPI-16 and BPI-17, those are ~4 m apart in a drift space section of Indus-2 lattice. The results are near to theoretical expectations and are shown in Figure T.1.23.

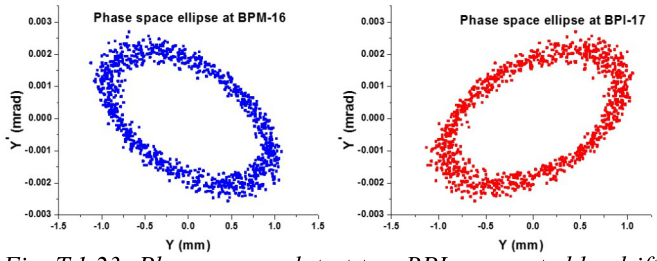

Fig. T.1.23: Phase space plot at two BPIs separated by drift space in Indus-2.

8. Conclusion

In conclusion, two pinger magnet systems have been successfully installed and commissioned in Indus-2 storage ring. These pinger magnets will be very useful tool in carrying out linear and nonlinear studies of the lattice parameters of Indus-2. In the preliminary experiments performed, turn-by-turn beam position data was collected for the first time using the vertical pinger magnet and analyzed for extracting the information related to linear beam optics in Indus-2. More experiments are planned in near future.

Acknowledgements

The authors sincerely thank Dr. Riyasat Husain, Shri Rahul Jain and Shri Yogesh Kelkar for their contribution towards initial experiments with pinger magnet system and analysis of turn-by-turn data. Authors also thank Shri Rajesh Kumar Agrawal, Shri K.V.A.N.P.S. Kumar and Shri Vinod Gaud for their contribution in the development of the pinger magnet sub-systems. The support provided by the other members of various contributing Divisions of RRCAT is also duly acknowledged. Indus operation crew members are also thankfully acknowledged for their support during the experiments with pinger magnet system.

References

[1] M. Pont, N. Ayala, G. Benedetti, M. Carla, Z. Marti, R. Nuñez "A Pinger Magnet System for the ALBA Synchrotron light source" 6th International Particle Accelerator Conference IPAC2015, Richmond, VA, USA.

[2] Deepak Kumar Tyagi and A. D. Ghodke, "Beam dynamics with pinger magnet in Indus-2 electron storage ring", in Proc. InPAC'18, IUAC, Delhi.

[3] M. Pont, R. Nunez, E. Huttel, "Septum and Kicker Magnets for the ALBA booster and storage ring" Proceedings of IPAC2011, San Sebastián, Spain.

[4] P. Lebasque, L. Cassinari, J.-P. Daguerre, C. Herbeaux, M.-P. Level, C Mariette, R. Nagaoka, "Optimization of coating thickness on the ceramic vacuum chambers of Soleil storage ring", in Proc. EPAC'2006, pp. 3514-3516.

[5] Bhardwaj V., Kumar P., Bairwa M. K., Singh R., Sindal B.K., Yadav D.P., Upadhyaya B.N., Bindra K. S. "Development of UHV compatible SS 316L-Kovar welding joint using fiber coupled pulsed Nd:YAG laser for accelerator applications" National Laser Symposium-29, Indore, Feb. 12-15, 2021.

[6] Pravin Fatnani, Anurag Bansal, Rajesh Kumar Agrawal, Kirti G. Barpande, Amit Chauhan, Sampa Gangopadhyay, Pankaj Gothwal, Ashesh Mangaldas Gupta, Musuku Janardhan, Bhavna Nitin Merh, Rohit Mishra, Kutubuddin Saifee, M Seema, Yogendra M Sheth, Bakshi Sanjai Kumar Srivastava, Rishipal Yadav, Status of Indus-2 Control System, 10th International Workshop on Personal Computers and Particle Accelerator Controls (PCaPAC-2014), 14 - 17 October 2014, Karlsruhe, Germany.

[7] M. Carlá, Z. Martí, G. Benedetti, Alba, Cerdanyola del Valles, Spain L. Nadolski, Soleil, Saint Aubin, France "Optimization of turn-by-turn measurements at SOLEIL and ALBA light sources" 6th International Particle Accelerator Conference IPAC2015, Richmond, VA, USA.

[8] P. Hartmann J. Fursch, D. Schirmer, T. Weis, K. Wille, "Experience with Libera Beam Position Monitors at Delta", Proceedings of DIPAC 2007, Venice, Italy.

[9] P. Castro, J. Borer, A. Burns, G. Morpurgo, R. Schmidt, "Betatron function measurement at LEP using the BOM 1000 turns facility", in Proc. PAC' 93, pp. 2103-2105.